royalsocietypublishing.org

Research

Article submitted to journal

Subject Areas:
xxxxx, xxxxx, xxxx

Keywords:
motile cilia, synchronization, metachronal waves

Author for correspondence:
Insert corresponding author name
e-mail: pc245@cam.ac.uk

Supplementary Materials to: Motile cilia hydrodynamics: Entrainment versus synchronisation when coupling through flow

Evelyn Hamilton[1], Nicola Pellicciotta[1], Luigi Feriani[1,2,3], and Pietro Cicuta[1]

[1]Cavendish Laboratory, University of Cambridge, JJ Thomson Av., Cambridge CB3 0HE, UK
[2]Institute of Clinical Sciences, Imperial College London, London W12 0NN, UK
[3]MRC London Institute of Medical Sciences, London W12 0NN, UK

This supplementary material provides details of methods and additional figures.

THE ROYAL SOCIETY PUBLISHING

(a) Phase-position transformation for power laws

The natural phase measures the phase in a moving frame such that the phase increases linearly for an uncoupled oscillator. The transformation to the natural phase is found by taking advantage of this definition:

$$\frac{d\phi}{dx_r} = \frac{d\phi}{dt}\frac{dt}{dx_r} \tag{S1}$$

$$= -\frac{2\pi}{2\tau_0}\left|\frac{\gamma}{F(x_r)}\right|, \tag{S2}$$

where π/τ_0 is the constant phase velocity for an isolated rower, τ_0 the time between successive trap updates i.e. the semi-period. The natural phase was chosen to be strictly decreasing for repulsive potentials. The transformation between ϕ and x_r is found by integrating the expression in eq. S2. Given the prevalence of power law driving potentials in this work, it is useful to directly state the transformation between phase and position for this case,

$$\phi(x) = (N_s+1)\pi + C_0 - \frac{\gamma\pi}{k\beta\tau_0}\frac{1}{2-\beta}x_r^{2-\beta}, \tag{S3}$$

$$C_0 = \frac{\gamma\pi}{k\beta\tau_0}\frac{x_s^{2-\beta}}{2-\beta} = \frac{\pi x_s^{2-\beta}}{(A+x_s)^{2-\beta}-x_s^{2-\beta}}\,. \tag{S4}$$

The parameters defining the driving potential β, x_s, τ_0, and A, are explained in section 2a of the main text. The counter N_s enumerates the number of trap updates that have taken place, which distinguishes between cases with $x_t > 0$ and $x_t < 0$. The constant C_0 ensures the switch point x_s is at $n\pi$, with $\phi \in [0,\pi)$ for $x_t > 0$ (rower moving right) and $\phi \in [\pi, 2\pi)$ for $x_t < 0$ (rower moving left). The initial N_s is chosen to be consistent with $\phi \in [\pi, 2\pi)$ for $x_t < 0$. This convention was introduced in our work in [1].

The two oscillators are not identical in this case, differently to [1]. Here one rower has been detuned by scaling the trap strength. Detuning through trap strength does not introduce any difference in the phase-position transformation. The transformation depends exclusively on the trap shape, switch point and amplitude. Consequently, the phase position transformation for power laws in eq. (S3) still holds. The force in terms of the phase does depend on which rower is being considered. The dependence stems from the trap strength, and so is a coefficient for the general trap structure $F_g(\phi_i)$,

$$F_n(x(\phi_n)) = k_n F_g(\phi_n) \tag{S5}$$

$$= k_n \begin{cases} \beta C_1^{-p}(\pi - C_0 - \phi_n)^{-p}, & 0 < \phi < \pi \\ -\beta C_1^{-p}(2\pi - C_0 - \phi_n)^{-p}, & \pi < \phi < 2\pi \end{cases}, \tag{S6}$$

$$C_1 = \frac{\pi}{(A+x_s)^{2-\beta} - x_s^{2-\beta}}, \quad C_0 = C_1 x_s^{2-\beta}, \quad p = \frac{1-\beta}{2-\beta}. \tag{S7}$$

The subscript n differentiates between the trap strength for the detuned rower, k_d, and the unaltered rower, k_u.

(b) Defining the average interaction between rower and signal

Restricting our focus to the direction of oscillation for the signal case, the position of the bead updates as

$$\frac{dx}{dt} = \frac{1}{\gamma}F(x) + V_{ext}(t). \tag{S8}$$

The rower is driven by a power law, i.e. the phase-position transformation defined in the previous section applies. There is no external flow applied when determining the phase-position transformation.

$$\frac{d\phi_R}{dt} = \frac{d\phi_R}{dx_r}\frac{dx_r}{dx}\frac{dx}{dt} \tag{S9}$$

$$= \Omega_R + \Omega_R \left|\frac{\gamma}{F(x)}\right| V_{ext}(t). \tag{S10}$$

The external velocity is a square wave, and so the time of the signal can be converted to a phase ϕ_S that is proportional to t. In this format the external signal is expressed as,

$$V_{ext}(\phi_S) = \begin{cases} v_{ex}, & 0 \le \phi_S < \pi \\ -v_{ex}, & \pi \le \phi_S < 2\pi \end{cases}, \qquad \frac{d\phi_S}{dt} = 2\pi f_e = \Omega_S. \tag{S11}$$

The frequency of the external signal f_e is detuned in this system, with the rower kept at a constant frequency. Using this expression it possible to express the evolution of the rower phase purely in terms of the two phases ϕ_R and ϕ_S. The interaction can then be averaged using the phase reduction method, with the same technique applied in [1],

$$\frac{d\phi_R}{dt} = \Omega_R + \Omega_R \left|\frac{\gamma}{F(x(\phi_R))}\right| V_{ext}(\phi_S) \tag{S12}$$

$$\approx \Omega_R + \frac{\Omega_R \gamma v_{ex}}{\pi |F(x_s)|} G_S[\psi_S], \tag{S13}$$

$$G_S[\psi_S] = \frac{\pi |F(x_s)|}{2\pi} \int_0^{2\pi} \text{sign}(V_{ext}(\theta)) \left|\frac{1}{F(x(\psi_S+\theta))}\right| \left.\frac{dx_r}{dx}\right|_{(\psi_S+\theta)} d\theta. \tag{S14}$$

To distinguish the phase difference with respect to the external signal the subscript S is included in ψ_S, similarly for the averaged interaction $G_S[\psi_S]$. Combining this expression with the phase velocity of the external flow gives an expression for the time derivative of the phase difference,

$$\frac{d\psi_S}{dt} = \Omega_R - \Omega_S + \frac{\Omega_R \gamma v_{ex}}{\pi |F(x_s)|} G_S[\psi_S]. \tag{S15}$$

$G_S[\psi_S]$ can be written explicitly in the power law case. The expression for the force in terms of phase is stated in eq. (S18), with the trap strength k_u, and the phase-position transformation is defined in eq. (S3). Evaluating the integral results in,

$$G_S[\psi_S] = \begin{cases} \frac{C_0^{-p}}{p+1}\left[C_0^{p+1} + (\pi + C_0)^{p+1} - 2(C_0 - \psi_S)^{p+1}\right], & -\pi < \psi_S \le 0 \\ \frac{C_0^{-p}}{p+1}\left[2(\pi + C_0 - \psi_S)^{p+1} - C_0^{p+1} - (\pi + C_0)^{p+1}\right], & 0 < \psi_S \le \pi \end{cases}. \tag{S16}$$

C_0 and p are the same as defined in eq. (S7).

(c) Dimensionless interaction between two detuned rowers

Applying the same technique to the detuned rower pairs, the time derivative of the rower phase can be calculated:

$$\frac{d\phi_n}{dt} = \Omega_n + \left.\left(\frac{d\phi}{dx_r}\frac{dx_r}{dx}\right)\right|_{\phi_n} \mu_{nn'} F_{n'}(x(\phi_{n'})) \tag{S17}$$

$$\approx \Omega_n + \frac{\tilde{\mu}_{nn'}}{\gamma}\frac{1}{2\pi}\int_0^{2\pi} \left.\left(\frac{d\phi}{dx_r}\frac{dx_r}{dx}\right)\right|_{\psi_{nn'}+\theta} F_{n'}(x(\theta))\, d\theta \tag{S18}$$

$$= \Omega_n + \tilde{\mu}_{nn'}\frac{\Omega_{n'}}{\pi} G_{ID}[\psi_{nn'}], \tag{S19}$$

$$G_{ID}[\psi] = \frac{1}{2}\int_0^{2\pi} \left.\left(\frac{dx_r}{dx}\right)\right|_{(\psi+\theta)} \left|\frac{1}{F_g(\psi_\theta)}\right| F_g(\theta)\, d\theta. \tag{S20}$$

In the expression above, the phase velocity of each bead is Ω_n, and the dimensionless hydrodynamic coupling term $\tilde{\mu} = \gamma\mu$. The evolution of the phase difference can be determined

using the phase derivatives, leading to the expression

$$\frac{d\psi}{dt} = \Omega_d - \Omega_u + \tilde{\mu}_{du}\left(\frac{\Omega_u}{\pi}G_{ID}[\psi] - \frac{\Omega_d}{\pi}G_{ID}[-\psi]\right), \tag{S21}$$

where we have set $\psi = \phi_d - \phi_u$.

(d) Compression of crescent trajectories to rower potentials

The crescent-shaped trajectories are found by fitting a second order Fourier series to the x and y tracking data. The fit is calculated using the inbuilt MATLAB `fit` function with the option `fourier2`. Each direction's fit specifies a frequency, these are then combined for the final trajectory by taking the average. The next step is to compress this path to one-dimension. This requires some definition for the end points where the direction is reversed. We chose the end points by considering the speed along the fitted path. First the local speed minima were selected as points of interest. If the number of interesting points is even, then the points with the largest and smallest x values were chosen as endpoints; the x direction is parallel to the epithelial cell wall. Alternatively if the number of interesting points was odd, the midpoint along the shortest segment was used as an end point. The two different cases are illustrated in figures S1(a) and S1(b).

The endpoints are used to calculate the central axis. This is the curve onto which the data points are then projected. The axis is calculated by separating the original path into upper and lower sections using the endpoints. Each segment is described by the same number of points that are equally spaced in time. The central line is found by pairing points on each trajectory using the time from the endpoint and finding the midpoint. Having found a central line, the data points are then mapped onto this curve by minimising the distance of each point to the curve. An example is shown in figure S1(c).

A rower trapping force potential is determined by fitting a curve to position and force data. The centre of drag position was compressed to one-dimension in the earlier steps. The process is simpler for the net force, which was calculated using the total force the cilium exerts on the fluid. To convert to one-dimension, the magnitude of the force is unchanged and the sign calculated using the angle with the central axis. Specifically the sign of the dot product between the force and the local direction of the central axis. If the change in the projected position and the projection of the force point in opposite directions on the central axis, the point is excluded. An example of the classification is shown in figure S1(d), where the red points indicate a positive force and the blue negative. The black crosses indicate points that are excluded. A rower trapping function can be found by fitting the position and force data. Note the traps were assumed to be attractive, consequently the distance is measured relative to a switching end. The trajectories and fitted potentials for each flagellum we tracked are shown in figures S2, S3, S4, S5, and S6.

(e) Compressing flagella trajectories (pseudocode)

Algorithm: Coarse graining flagella onto rotors' trajectory, and trajectory compression

Track the cilium:

- Load the high speed microscopy video of cilia beating
- **foreach** *frame to track* **do**
  - Track the cilium by clicking on several points along the snapshot of the cilium
  - Interpolate the clicked points to have a smooth representation of the cilium

Coarse-grain the cilium beat pattern as a rotor:

- **foreach** *tracked configuration of the cilium (at time t)* **do**
  - Approximate cilium with N cylinders $1\,\mu\mathrm{m}$ long
  - Approximate next tracked cilium (at time $t + \Delta t$) with N cylinders $1\,\mu\mathrm{m}$ long
  - **foreach** *cylinder approximating the cilium at time t* **do**
    - Measure the displacement of its midpoint
    - Measure its velocity along the directions parallel and perpendicular to its axis
    - Use RFT to find the force the cylinder exerts on the fluid in moving to its position at $t + \Delta t$
  - Integrate the force contributions, taking into account overlapping cylinders. This yields the total force exerted by the cilium
  - Average of the position of the N cylinders approximating the cilium configuration, weighting by the magnitude of the force they exert on the fluid. This yields the position of the effective "centre of drag" of the cilium
- A colloidal rotor following the trajectory of the centre of drag of the cilium coarse-grains effectively the beat pattern of the tracked cilium.

Preprocess the position and force data:

- Load the trajectory data
- Translate the trajectory to be centered on (0,0)
- Convert to microns from pixels
- **if** *crescent trajectory* **then**
  - Set the convention that the x direction is parallel to the cell wall
  - Select only complete cycles

Fit a trajectory to the centre of drag positions:

- **if** *elliptical trajectory* **then**
  - Fit an ellipse to the position data
- **else if** *crescent trajectory* **then**
  - Fit a second order Fourier series to both x and y

Compress the position data to one-dimensions:

- **if** *elliptical trajectory* **then**
  - Rotate the ellipse to align the major axis with the x axis
  - Set the compressed position to the new x position
- **else if** *crescent trajectory* **then**
  - Define the central axis
  - Find the points of minimum speed along the orbit
  - Set end points to the minima that maximise the separation relative to the cell wall
  - **if** *odd number of minima* **then**
    - Find the midpoint along the short arc
    - Set as new end point
  - Set the inner and outer segments of the crescent using the endpoints
  - Set the central axis by finding the midpoints between each segment:
    - Sample the inner and outer segments equally over time
    - Pair points by time to travel to endpoint (use the negative time for the inner)
    - Find the midpoint of the pairs
  - Project data onto the central axis by minimising the distance to the trajectory

Compress the force data to one dimension:

- Set the magnitude of the compressed force to the magnitude of the measured force
- Set the sign/direction of the force using the fitted trajectories
- **if** *elliptical trajectory* **then**
  - Use the major axis to group the data into positive and negative forces. With points on same side having the same direction
- **else if** *crescent trajectory* **then**
  - Find the change in the compressed position
  - Find the cosine of direction of the force relative to the central axis
  - Exclude points that don't match in these measures
  - Set force direction using sign of the change in compressed position

Transform the compressed position data to be measured relative to the end point it is approaching (i.e. the compressed position should always be decreasing with time, and the traps are attractive)

Find the force-position relationship by fitting a function (cubic polynomial) to the compressed force and compressed position data

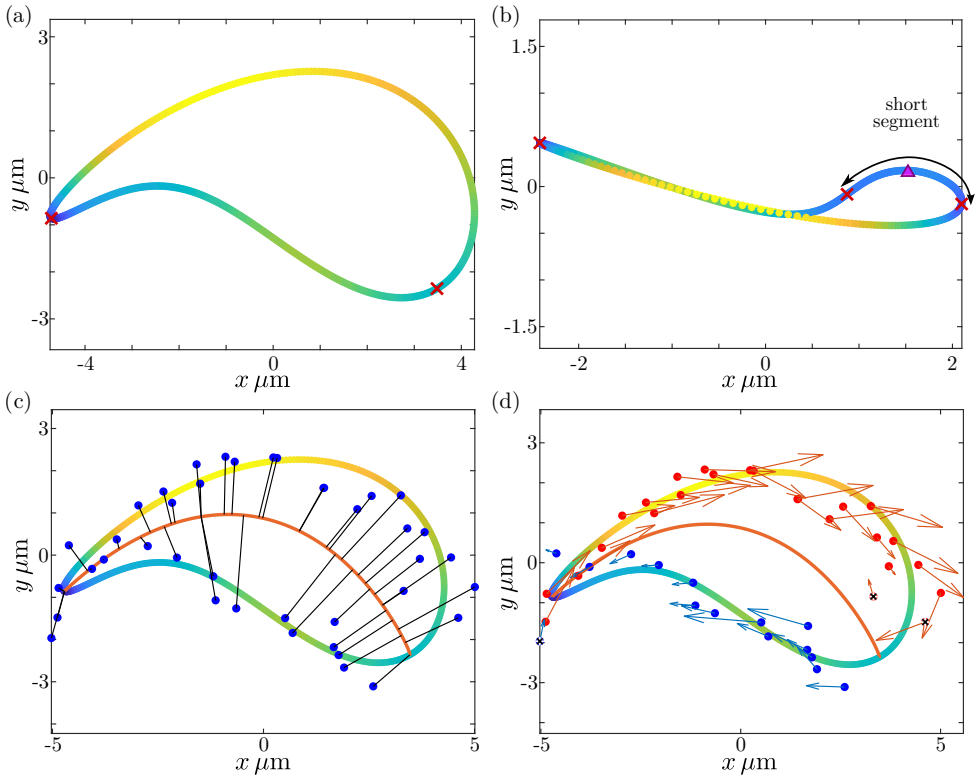

Figure S1. Illustrations of certain steps for compressing the crescent shaped trajectories into rower potentials. (a) Classifying endpoints when there are an even number of points. Local minima in the speed are marked by red crosses, with the colour of the trajectory indicating the speed. The two values with the most extreme x values are selected as endpoints. In this case there are only the two. (b) When the number of minima is odd, the centre of the shortest segment is used as one of the endpoints. (c) The centre of drag data is compressed to one-dimension by finding the shortest path to the central axis. Here the data are the blue dots, and the black lines indicate the projection. (d) The forces are classified as positive or negative depending on their alignment. Red points have a positive sign and blue points are negative. If the change in position is contradictory to the force alignment the point is marked with a black cross and excluded.

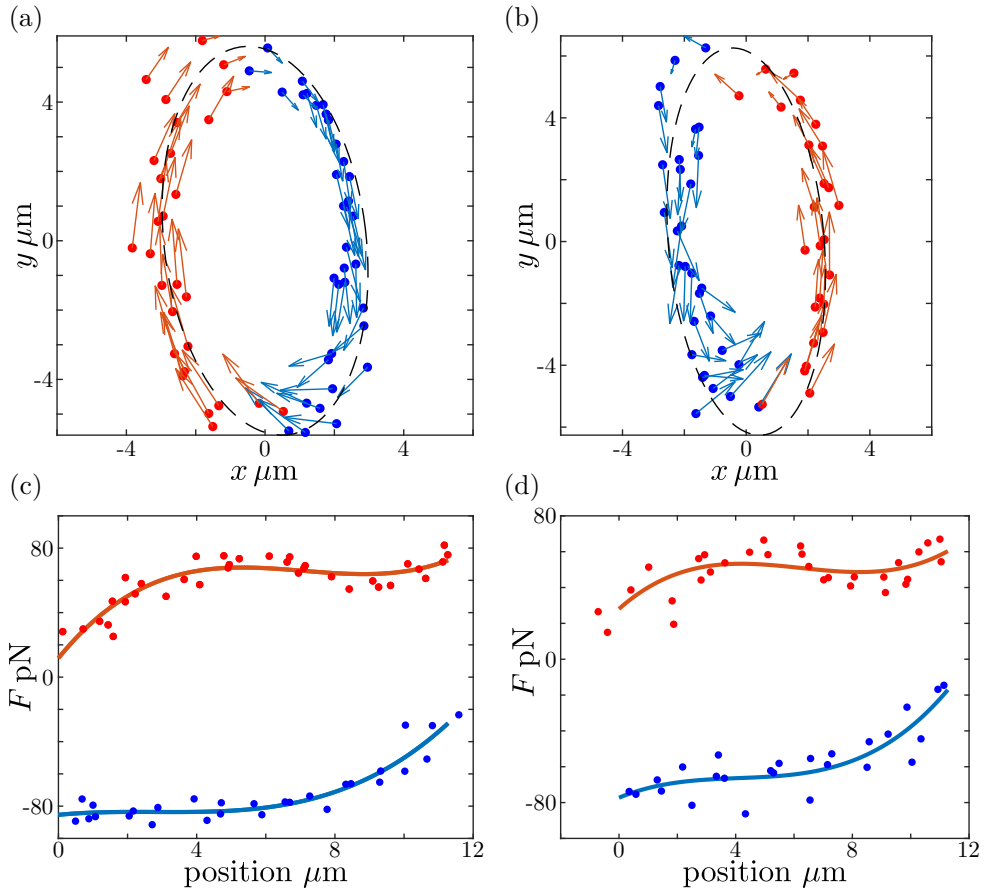

Figure S2. Converting trajectories of *Chlamydomonas* flagella into rower force profiles. The source videos are from [2]. (a,b) The trajectories of the left and right flagella. The points are grouped using the major axis of the fitted ellipse. Values on the inside half are blue and set as negative, while points on the outside are red and assigned a positive value. (c,d) The force profiles fit to the centre of drag trajectories. To position the points, the distance parallel to the major axis is used. The position here is equivalent to the distance relative to the trap for rowers, and is strictly decreasing following the trajectory. Consequently the position of the blue points is measured relative to the bottom of the ellipse, and the red points from the top.

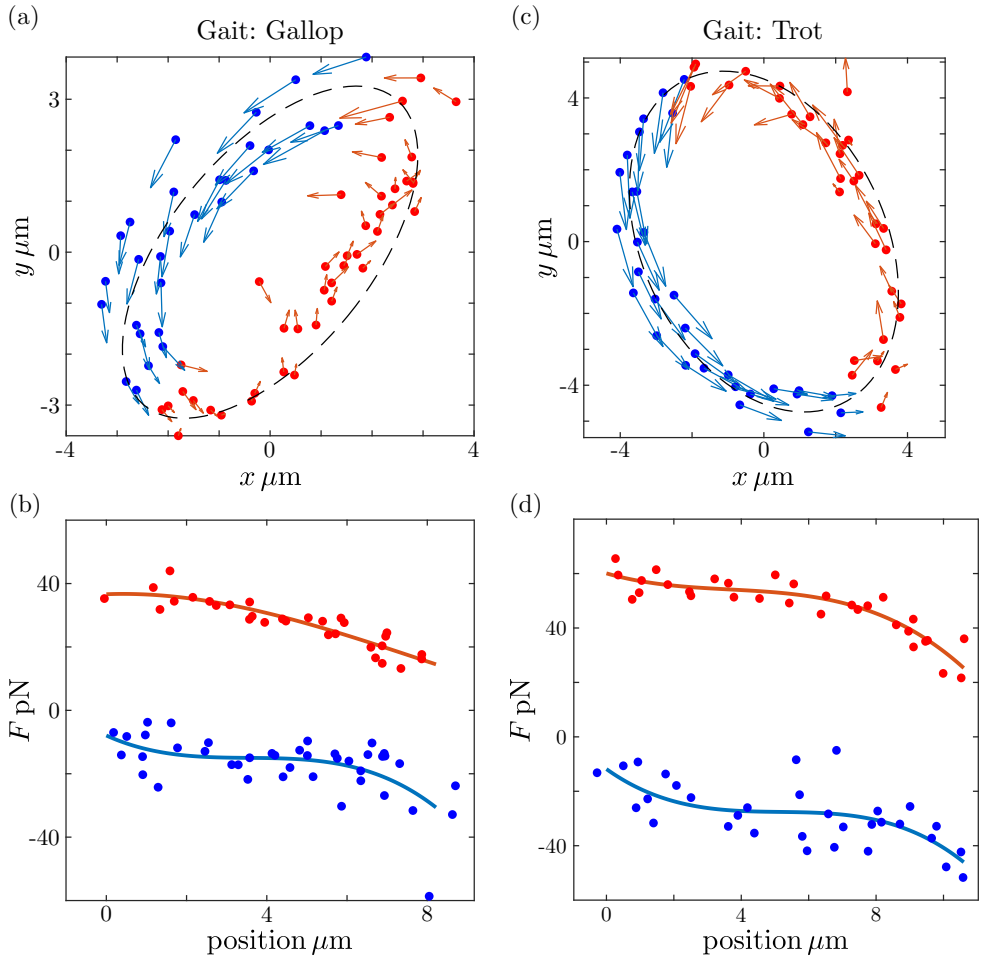

Figure S3. Force profiles determined using the motion of quadri-flagellated algae, source [3]. (a) The trajectory and profile when the algae is in "gallop gait". (b) The force profile is calculated using the same approach as *Chlamydomonas*. (c) The trajectory for a flagellum when alga is exhibiting the trot gait. (c) The force profile calculated for the trot gait.

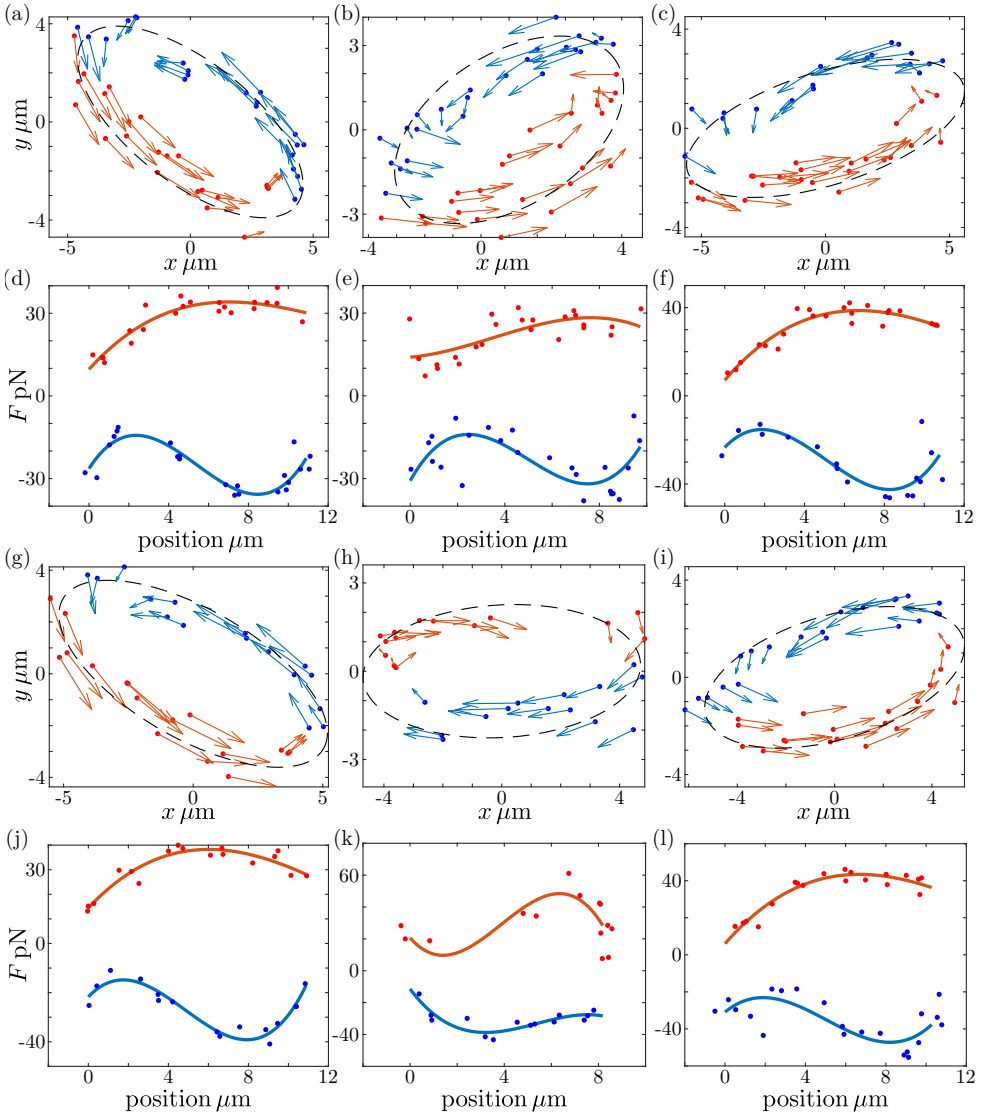

Figure S4. Force profiles determined using the flagellum motion of *Volvox* cells. The videos from [4] where one flagellum was snipped were used for this calculation. The remaining flagellum was tracked, which reduced the error.

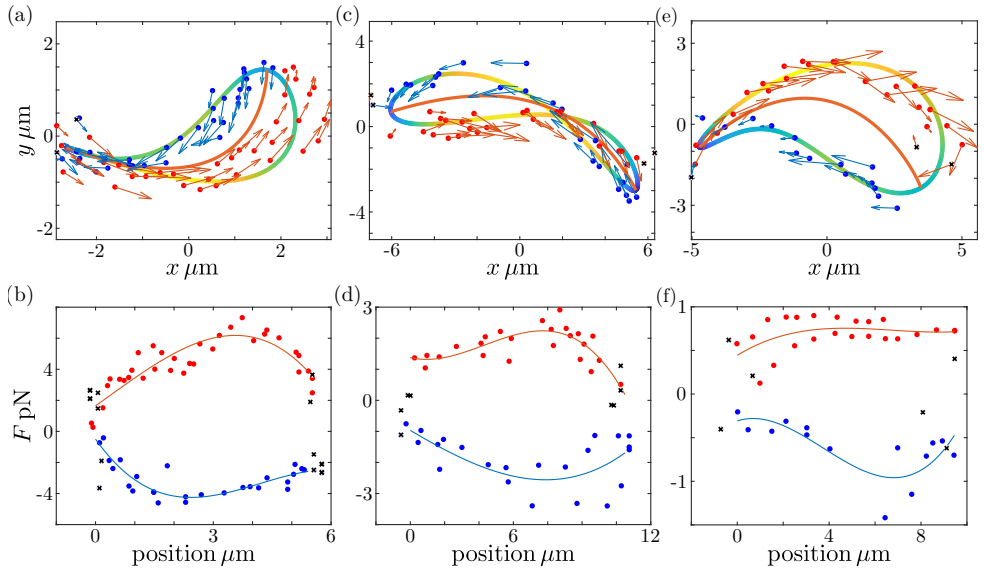

Figure S5. Trajectories and force profiles derived using the other mouse cilia. (a) Trajectory of the centre of drag calculated from [5]. (b,c) Trajectories from videos of ependymal cilia from mouse brain *in vivo* [6].

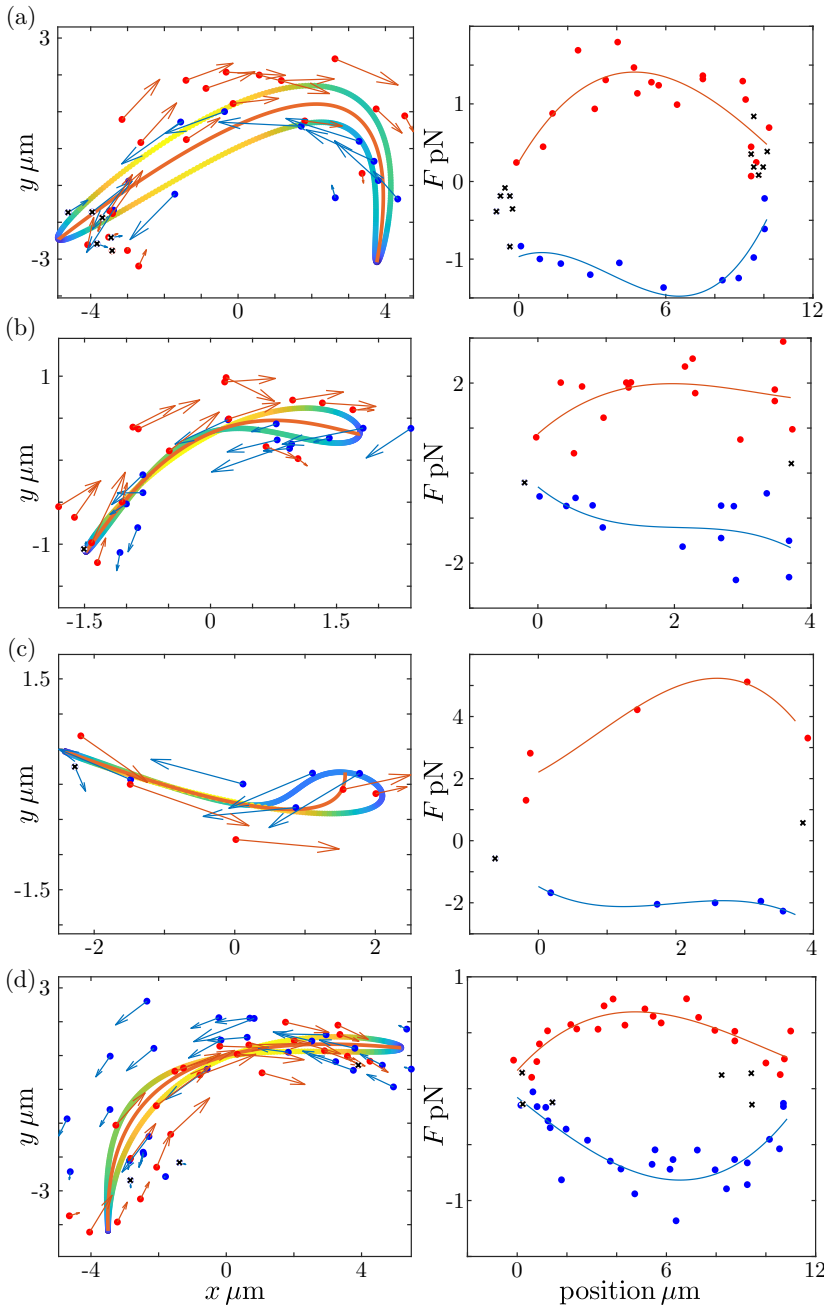

Figure S6. Rower force profiles derived from trajectories of the centre of drag describing cilia in human airways [7].

References

1. Hamilton E, Cicuta P. 2018 Interpreting the synchronisation of driven colloidal oscillators via the mean pair interaction. *New J. Phys.* **20**, 093028.
2. Wan KY, Goldstein RE. 2014 Rhythmicity, recurrence, and recovery of flagellar beating. *Phys. Rev. Lett.* **113**, 238103.
3. Wan KY, Goldstein RE. 2016 Coordinated beating of algal flagella is mediated by basal coupling. *Proc. Natl. Acad. Sci. U.S.A.* **113**, E2784–E2793.
4. Brumley DR, Wan KY, Polin M, Goldstein RE. 2014 Flagellar synchronization through direct hydrodynamic interactions. *eLife* **3**.
5. Pellicciotta N, Hamilton E, Kotar J, Faucourt M, Spassky N, Cicuta P. 2019 Synchronisation of mammalian motile cilia with hydrodynamic forces. *Submitted*.
6. Lechtreck KF, Delmotte P, Robinson ML, Sanderson MJ, Witman GB. 2008 Mutations in Hydin impair ciliary motility in mice. *J Cell Biol* **180**, 633–643.
7. Chioccioli M, Feriani L, Nguyen Q, Kotar J, Dell SD, Mennella V, Amirav I, Cicuta P. 2019 Quantitative high speed video profiling discriminates between variants of primary ciliary dyskinesia. *Am. J. Resp. Crit. Care Med.*